



Published in final edited form as:

*Br J Surg*. 2011 December ; 98(12): 1725–1734. doi:10.1002/bjs.7698.

## Predicting the Survival of Ischaemic Bowel in Preclinical Model Systems using Intraoperative Near-Infrared Fluorescence Angiography

Aya Matsui, M.D.<sup>1,2</sup>, Joshua H. Winer, M.D.<sup>3</sup>, Rita G. Laurence, B.S.<sup>1</sup>, and John V. Frangioni, M.D., Ph.D.<sup>1,4</sup>

<sup>1</sup>Division of Haematology/Oncology, Beth Israel Deaconess Medical Centre, Boston, MA

<sup>2</sup>Division of Cancer Diagnostics and Therapeutics, Hokkaido University Graduate School of Medicine, Sapporo, Japan

<sup>3</sup>Department of Surgery, Brigham & Women's Hospital, Boston, MA

<sup>4</sup>Department of Radiology, Beth Israel Deaconess Medical Centre, Boston, MA

### Abstract

**Background**—Predicting the long-term viability of ischaemic bowel during surgery is challenging. We hypothesized that intraoperative near-infrared (NIR) angiography (NIR-AG) of ischaemic bowel might provide metrics that were predictive of long-term outcome.

**Materials and Methods**—NIR-AG using indocyanine green (ICG) was performed on N = 24 pigs before and after inducing bowel ischaemia to determine the feasibility of NIR-AG to detect compromised perfusion. Contrast-to-background ratio (CBR) over time was measured in regions of interest throughout the bowel, and various metrics of the CBR-time curve were developed. N = 60 rat bowels, with or without strangulation, were imaged intraoperatively and on postoperative day (POD) 3. CBR metrics and clinical findings obtained intraoperatively were assessed quantitatively for their ability to predict animal survival, histological grade of ischaemic injury, and visible necrosis at POD 3.

**Results**—In the ischaemic bowels of pigs, various qualitative and quantitative CBR metrics appeared to correlate with bowel injury as a function of distance from normal bowel. In rats, intraoperative clinical assessment showed high specificity but low sensitivity for predicting outcome on POD 3. Qualitative patterns of the CBR-time curve, such as absence of an arterial inflow peak and presence of a NIR filling defect, resulted in better accuracies to predict animal survival, histological grade, and visible necrosis at POD 3 of 90%, 85% and 92%.

---

\*To whom all correspondence should be addressed: John V. Frangioni, M.D., Ph.D., BIDMC, Room SL-B05, 330 Brookline Avenue, Boston, MA 02215, 617667-0692 FAX: 617-667-0981, jfrangio@bidmc.harvard.edu.

#### **Author Statements of Financial Interest:**

Aya Matsui, M.D.: None

Joshua H. Winer, M.D.: None

Rita G. Laurence, B.S.: None

John V. Frangioni, M.D., Ph.D.: All FLARE™ technology is owned by Beth Israel Deaconess Medical Center, a teaching hospital of Harvard Medical School. As inventor, Dr. Frangioni may someday receive royalties if products are commercialized. Dr. Frangioni is the founder and unpaid director of The FLARE™ Foundation, a non-profit organization focused on promoting the dissemination of medical imaging technology for research and clinical use.

**Devices Used:** Custom-built intraoperative near-infrared fluorescence imaging system with simultaneous color video and near-infrared fluorescence capabilities.

**Drugs Used:** Indocyanine Green (Sigma-Aldrich, St. Louis, MO).

**Conclusion**—Bowel survival at POD 3 can be predicted by intraoperative NIR-AG with higher accuracy compared to clinical evaluation alone. NIR-AG may someday prove useful clinically for avoiding unnecessary resection.

### Keywords

Bowel ischaemia; bowel infarction; near-infrared fluorescence; indocyanine green

## INTRODUCTION

The intraoperative assessment of bowel perfusion is typically subjective; therefore, surgeon experience is of paramount importance. Clinical findings, such as colour, pulsation, temperature, and/or peristalsis are the metrics that currently guide the extent of bowel resection in the presence of ischaemia. Unfortunately, clinical findings alone often lead to extensive bowel resections<sup>1</sup> or anastomotic failure.<sup>2</sup> The incidence of anastomotic leakage in gastrointestinal tract surgery, for example, has been reported to be 2.7% to 7.6% in recent studies.<sup>3–5</sup>

Matsui et al.<sup>6</sup> and others<sup>7–9</sup> have recently shown that intraoperative near-infrared (NIR) fluorescence angiography (NIR-AG) of perforator vessels can predict skin flap outcome on postoperative day (POD) 3. The contrast agent used in these studies was indocyanine green (ICG), a blood pool agent FDA-approved since 1958 for other indications. After rapid bolus injection, ICG sequentially highlights arteries, capillaries and veins, and permits precise mapping of tissue vascularity over time. In these studies, vascular flow served as a reliable surrogate for tissue perfusion.

After intravenous injection, ICG rapidly binds to plasma proteins and is cleared by the liver with a 2 to 4 min half-life.<sup>10</sup> This rapid elimination from blood makes ICG useful for angiography because results are available immediately and injections can be repeated every 10 to 20 min to avoid dose stacking. The hypothesis guiding this study was that NIR-AG of bowel, as it has been shown in skin,<sup>11</sup> might provide qualitative and/or quantitative intraoperative metrics that could predict clinical outcome on POD 3.

## MATERIALS AND METHODS

### NIR Fluorescence Imaging System

The Fluorescence-Assisted Resection and Exploration (FLARE™) NIR imaging system used in this study has been described in detail previously.<sup>12</sup> Briefly, the system is positioned using an articulated arm anywhere over the surgical field, with a working distance of 45 cm above the subject. White (400–650 nm) light and NIR fluorescence excitation (745–779 nm) light are generated by light emitting diodes (LED) over 15-cm diameter projection. Colour video (i.e., surgical anatomy) and NIR fluorescence (i.e., fluorophore distribution) images are achieved simultaneously via custom-designed optics. After computer-controlled camera acquisition via custom software, anatomic (colour video) and functional (NIR fluorescence) images can be displayed individually and merged. For merged images, the grayscale NIR fluorescence image was pseudo-coloured in lime green and superimposed on the colour video image. All images were refreshed up to 15 times per s. Hands-free operation utilizing motorized zoom and focus lenses and a foot-switch are also provided. Fluorescence intensity of any desired region of interest (ROI) was quantified using a 12-bit pixel scale (range, 0 to 4095).

## Animals

Animals were studied under the supervision of an approved institutional protocol. Female Yorkshire pigs (E. M. Parsons and Sons, Hadley, Massachusetts) weighing 33.1 to 42.3 kg (median; 37.6 kg) were induced with 4.4 mg/kg intramuscular Telazol, intubated, and maintained with 2% isoflurane (Baxter Healthcare Corp., Deerfield, Illinois). Male 250-g Sprague-Dawley rats from Charles River Laboratories (Wilmington, MA) were induced and maintained with isoflurane.

### NIR-AG of Ischemic Porcine Bowel

A total of N = 24 pigs were included in the study. Pigs were chosen for initial optimization of the technology because the size, thickness, chromophore content, and scattering coefficients of their bowel closely resemble those of humans, providing potential for immediate clinical translation of the results. A standard midline laparotomy was performed and the small bowel was exposed. To create an ischaemic segment, mesenteric vessels were isolated. After a 30 min waiting period to avoid possible vascular spasm following this dissection, animals underwent initial NIR-AG using a rapid intravenous bolus injection of 0.05 mg/kg ICG (Akorn, Decatur, IL). Because the mesenteric vessels of pig small bowel are branched more proximally than the vessels of human and there are fewer communicating vessels, the ischaemic segment is well-defined after clamping. Thus, it was easy to create different lengths of ischaemia by adjusting the number of mesenteric vessels that were clamped. The extent of the ischaemia was expected to be more severe at the central part of the ischaemic segment. This model was created to mimic bowel anastomosis, and the mesenterium was trimmed to provide seam allowance even though the continuity of the bowel was not interrupted. Using this model, one can investigate perfusion as a single factor, eliminating the impact of the anastomotic technique.

Animals were then divided into 3 groups (N = 8 animals per group) based on the length of ischaemic segment created by mesenteric vascular occlusion using a vascular clamp (Figure 1A). Short (2–3 cm), medium (4–5 cm) and long (6–12 cm) ischaemic segments were defined, and each ischaemic segment was subdivided into equally spaced 2, 4 or 6 smaller segments ranging from 1 to 2 cm each (Figure 1A and Supplementary Tables S1 and S2). A numbered region of interest (ROI) was drawn on the border of the subdivided segment and adjacent non-ischaemic bowel at the mesenteric and anti-mesenteric side. The ROI was grouped according to the distance from normal bowel (Supplementary Tables S1 and S2). Isolated mesenteric vessels were occluded for the time indicated then, after the occlusion was removed, a second NIR-AG using ICG was performed. Camera exposure time for each individual image was fixed at 60 ms, and images were acquired in rapid succession for 10 min, creating a cine of the angiography. Fluorescence intensity of the ROI and background fluorescence were quantified and contrast-to-background-ratio (CBR) defined as (mean fluorescence intensity of ROI - mean fluorescence intensity of background)/(mean fluorescence intensity of background). Maximum fluorescence intensity ( $I_{\max}$ ) and fluorescence intensity at 120 s (2 min) postinjection ( $I_{120}$ ) were defined, and the drainage ratio was calculated as  $I_{120}/I_{\max} \times 100$ .

### NIR-AG of Ischemic Rat Bowel

A total of N = 60 rats were included in the study. Rats were chosen for the survival studies because a large number was needed to test all clinical parameters with high statistical accuracy. The abdomen of the anesthetized animals was shaved and swabbed with betadine. A 0.7 cm midline laparotomy was performed using sterile technique. The small bowel was gently retrieved from the abdominal cavity and points at 10 and 20 cm (oral side) from the ileum end were marked with a sterile marker. In N = 50 animals, the bowel segment between the 2 marked points was strangulated using a vascular occluder (Model VO-1.5,

DocXS, Ukiah, CA) having a lumen size of 1.5 mm and cuff pressure of 1.0 atm. Duration of the strangulation was 0.5 h (N = 14), 1 h (N = 12), 2 h (N = 12) and 4 h (N = 12). After removal of the occluder, the affected bowel segment, along with a minimum of 1 cm of unaffected bowel on both the oral and anal sides, was exposed and imaged by NIR-AG after rapid intravenous injection of 0.15 mg/kg ICG. Data acquisition was performed as described above for the pig experiments. N = 10 animals served as control, undergoing sham surgery without strangulation.

After imaging, the bowel segment was returned to the abdominal cavity, which was sutured shut. Animals were allowed to recover from anaesthesia in a separate cage, and singly housed for 3 d. A duration of 3 d was chosen because rat tissues and organs are relatively resistant to apoptosis and/or necrosis from ischemia and by 3 d irreversible tissue injury had occurred. Buprenorphine hydrochloride (Hospira, Inc., Lake Forest, IL) was administered subcutaneously at closure of the abdomen and on POD 1. On POD 3, animals were re-anesthetized and underwent repeat NIR-AG as described above. Animals that died before the second laparotomy failed to receive repeat NIR-AG, and an autopsy was performed immediately after death.

### CBR-Time Curve Parameters and Assessment of Clinical Outcomes

The bowel was equally subdivided into 5 sub-segments in the strangulation groups and 4 sub-segments in the control group. On the day of surgery (DOS) and on POD 3, each sub-segment was labelled by a blinded observer as either viable or nonviable. Clinical assessment included colour, pulsation and peristalsis. ROIs over each sub-segment were used to measure CBR and drainage ratio, as described in detail above. Drainage ratio and maximum fluorescence intensity in affected segments were compared to the controls. Bowel specimens were harvested immediately after NIR-AG and immediately before sacrifice, fixed with 3% paraformaldehyde, and processed for hematoxylin and eosin (H&E) staining. Microscopic criteria described by Park, et al.,<sup>13</sup> as originally developed by Chiu, et al.<sup>14</sup> was used for histological assessment on a scale ranging from 0 to 8 (Supplementary Table S3).

Clinical assessment, visual distribution of NIR fluorescence, presence or absence of an arterial inflow peak in the CBR curve, and other patterns of the CBR-time curve on DOS were evaluated for accuracy in predicting animal survival, unfavourable histological grade and visible necrosis at POD 3. Receiver operating characteristic (ROC) curves of maximum fluorescence intensity to control, drainage ratio, and drainage ratio to control were generated, and the area under the curve (AUC) was obtained. The point on the ROC curve that maximized sensitivity and specificity was assigned as the cutoff value for subsequent analysis.

### Statistical Analysis

In the rat bowel strangulation models, the Mann-Whitney test or Wilcoxon matched pairs test was employed to determine statistical difference between the 2 groups, and the Kruskal-Wallis one-way analysis of variance was used for multiple groups. Accuracy of each assessment to determine the viability of ischaemic bowel was presented by Fisher's exact test. Analysis was performed using Prism 4 (GraphPad Software, San Diego, CA) with two-sided 95% confidence intervals. Analyzed values were presented as mean  $\pm$  SD.

## RESULTS

### NIR Fluorescence Angiography (NIR-AG) of Normal and Ischaemic Pig Bowel

Typical NIR-AG images seen under normal and ischaemic conditions are shown in Figure 1A. In the setting of mesenteric vascular occlusion, a major filling defect was obvious in the

NIR fluorescence image, but changes in the colour video image were much more subtle. Visible fluorescence intensity and time to fluorescence filling was found to be a function of ischaemic length (data not shown). In 4 of 8 animals in the long ischaemia segment group, the centre of the ischaemic segment had a sustained filling defect by NIR-AG.

Analysis of the CBR-time curve in normal and ischaemic bowel revealed 4 possible patterns (Figure 2A), which permitted quantitation of certain metrics (Figure 2B). Normal, non-ischaemic bowel had a sharp and high ( $\geq 25\%$  of the plateau) arterial inflow peak followed by rapid decline to a relatively steady plateau level of NIR fluorescence. Prior to vascular occlusion, all  $N = 336$  sub-segments showed this normal arterial pattern. The delayed drainage pattern also had an arterial inflow peak, but rather than the signal decaying over time, NIR fluorescence signal intensity actually increased over time. Based on prior studies, delayed drainage was present when drainage ratio  $\geq 85\%$ . The capillary pattern had an absent arterial inflow peak and a slow rise of CBR over time. The arterial insufficient pattern corresponded to a static defect in NIR fluorescence, with no change in CBR from baseline after ICG injection. In the 336 subsegments of bowel analyzed, the arterial, delayed drainage, capillary, and arterial insufficient patterns present were found in 177 (52.7%), 73 (21.7%), 75 (22.3%) and 11 (3.3%), respectively. As shown in Supplementary Table S2, capillary and arterial insufficient patterns were frequently observed in ischaemic bowel sub-segments as a function of distance from normal bowel. Interestingly, the delayed drainage pattern appeared in areas adjacent to those showing compromised perfusion patterns, such as the capillary and arterial insufficient (Supplementary Table S2). In the short (2 to 3 cm) ischemic segment group, the inflow peak was retained even at the central part of ischaemia. The model used was convenient not only for examining the ability of NIR-AG to show the degree of ischemia by altering patterns of CBR-time curve, but also to show how long the capillary blood flow could perfuse the intestinal segment by itself.

### **NIR-AG in a Rat Bowel Strangulation Model**

Shown in Figure 1B are typical imaging results from the rat small bowel strangulation model. In the example shown, all 5 ischaemic subsegments were considered nonviable intraoperatively by clinical assessment, and 4 of 5 subsegments (ROIs 1, 2, 4, and 5) had a visible filling defect by NIR-AG. By POD 3, massive necrosis was seen in the colour video image, consistent with the filling defect seen on DOS (see also Supplementary Figure S1).

The duration of strangulation had a major impact on animal survival, histological grade of tissue damage, and the perfusion pattern seen by NIR-AG (Supplementary Figure S2). The presence or absence of strangulation (Supplementary Figure S3) and duration of strangulation (Supplementary Figure S4) also impacted the NIR-AG quantitative metrics maximum fluorescence intensity to control, drainage ratio and drainage ratio to control.

### **Predictive Capability of Intraoperative Clinical Assessment or NIR-AG Qualitative Patterns on Animal Survival, Histological Grade, and Tissue Necrosis at POD 3**

The sensitivity, specificity and accuracy of intraoperative clinical assessment for predicting animal survival, histological grade and tissue necrosis is detailed in Table 1. Although sensitivity was high (93%–100%) in all cases, specificity and therefore accuracy were low (47%–70%). Three qualitative NIR-AG patterns, however, showed improved predictive capability. The simple presence or absence of a visual filling defect (see, for example, Figure 1), resulted in a 77%, 85% and 92% accuracy in predicting animal survival, histological grade, and clinical necrosis, respectively on POD 3. The absence of an arterial inflow peak in the CBR-time curve improved accuracy to 90%, 85% and 85%, respectively. The arterial insufficient pattern had lower average sensitivity than did absence of an arterial inflow peak, but improved accuracy over clinical assessment, showing 88%, 79% and 76%,



respectively. A summary of the number of subsegments found under each condition is shown in Figure 3.

### **Predictive Capability of Intraoperative Quantitative CBR-Time Curve Metrics on Animal Survival, Histological Grade and Tissue Necrosis at POD 3**

Interestingly, the quantitative CBR-time curve metrics suggested that maximum fluorescence intensity to control, drainage ratio, and drainage ratio to control (Table 2) were inferior to all qualitative metrics and roughly equivalent to clinical assessment in terms of accuracy to predict intraoperatively the status of animal survival, histological grade and tissue necrosis on POD 3.

## **DISCUSSION**

Achieving adequate tissue perfusion is of paramount importance in bowel surgery. Because clinical decision making is currently performed using rather subjective clinical criteria, this study focused on the use of NIR-AG, with the goal of finding one or more reproducible metrics that could predict, intraoperatively and with high accuracy, long-term outcome with respect to animal survival, histological grade of tissue damage, and the presence of tissue necrosis.

Pig small bowel does not have well-developed collaterals among mesenteric vessels. The extent of vascular occlusion is therefore directly proportional to the final length of ischaemic bowel, providing a reliable model system. And, because the size and optical properties of pig bowel closely resemble the human bowel, preclinical validation of the technology will have immediate clinical relevance. Using this model system, short (2–3 cm) segments of mesenteric ischaemia did not alter the CBR-time curve compared to non-ischaemic bowel. Beyond 4 cm of ischaemia, however, the arterial inflow peak was lost. This is consistent with previous findings using perforator flaps, where perfusion was found to be a function of distance from the feeding vessel. Of note, due to the penetration depth of NIR light, NIR-AG provided direct visualization of all vessels, even when embedded in mesentery (see, for example, Figure 1A), similar to results provided by conventional X-ray angiography.

After defining the 4 vascular flow patterns seen under normal and ischaemic conditions in pig, a rat small bowel strangulation model was used to compare the sensitivity, specificity, and accuracy of various metrics for their ability to predict long-term outcome with clinical evaluation. Not surprisingly, clinical assessment alone had relatively low specificity and accuracy for predicting various clinical outcomes, with prediction of animal survival being no better than a coin toss (Table 1). In contrast to previously published work on skin flaps,<sup>6</sup> the quantitative metrics maximum fluorescence intensity to control, drainage ratio, and drainage ratio to control were only marginally better than clinical assessment (Table 2). The reasons for this are unclear, but suggest that when assessing bowel perfusion, newer quantitative metrics need to be developed.

Nevertheless, 3 simple qualitative metrics were found to be highly accurate when predicting clinical outcome on POD 3 from a single intraoperative measurement (Table 1): visual NIR fluorescence filling defect, absence of an arterial inflow peak, and the arterial insufficient pattern. The time required to acquire these metrics ranged from 60 ms to 120 s. Separately, each metric provided accuracies ranging from 77% to 90%, 79% to 85% and 76% to 92% for predicting animal survival, histological grade of tissue damage, and clinical necrosis, respectively. Using only the presence of a NIR filling defect to predict clinical necrosis and absence of the arterial inflow peak to predict animal survival and histological grade, accuracies of 90%, 85% and 92%, respectively were achieved.

Numerous techniques, including Doppler ultrasound,<sup>15</sup> laser tissue blood flowmetry,<sup>16</sup> near-infrared spectroscopy,<sup>17</sup> charged-couple device (CCD) microscopy,<sup>18</sup> pulse oximetry,<sup>19</sup> and fluorescence angiography using fluorescein injection<sup>20</sup> have been evaluated for clinical use during bowel surgery. Although fluorescein angiography was shown to be superior to Doppler ultrasound,<sup>21,22</sup> this optical technique is not currently used because visible fluorescence emission requires that all other operating room lights be off. Additionally, time to complete an examination was relatively long and repeat examination was hindered by fluorescein's long half-life for elimination. The technology we describe for bowel assessment can be translated rapidly to the clinic for testing because NIR-AG can be performed under NIR-depleted white light using the FLARE™ imaging system, NIR light penetration depth is several millimetres, ICG is cleared in minutes via circulation, and the entire measurement process takes only 2 min. Indeed, there are now several NIR imaging systems available for clinical studies (reviewed in<sup>23</sup>) as well as a major, previously reported, trial supporting the hypothesis presented in this study. Kudzusz et al.<sup>24</sup> showed in 402 patients undergoing elective colorectal surgery that NIR-AG evaluation of tissue perfusion at the site of anastomoses could halve the rate of most post-operative complications, and reduce the rate of leakage from hand-sewn anastomoses by 84%.

The present study must be interpreted, however, in the context of its limitations. First, vascular occlusion was utilized to induce ischaemia, but many clinical situations were caused by non-occlusive processes. The predictive capability of the metrics we describe under these conditions is unknown. Second, the metrics were not tested in the context of anastomosis, which can cause local changes in perfusion that could alter the accuracy of the metrics. Third, the safety margin (in cm) to ensure that anastomosed bowel segments remain viable has yet not been defined. Lastly, we have not yet found reproducible quantitative metrics that would remove all ambiguity about clinical decision making. Nevertheless, this study should lay the foundation for future preclinical and clinical studies.

## Supplementary Material

Refer to Web version on PubMed Central for supplementary material.

## Acknowledgments

**Funding:** This work was funded by National Institutes of Health grants R01-EB-005805 and R01-CA-115296.

We thank Lindsey Gendall for editing and Eugenia Trabucchi for administrative assistance. This work was funded by the National Institutes of Health grants #R01-EB-005805 and R01-CA-115296 to JVF.

**Sources of Funding:** National Institutes of Health grants #R01-EB-005805 and R01-CA-115296 to JVF.

## References

1. La Hei ER, Shun A. Intra-operative pulse oximetry can help determine intestinal viability. *Pediatr Surg Int.* 2001; 17(2–3):120–121. [PubMed: 11315268]
2. Karliczek A, Harlaar NJ, Zeebregts CJ, Wiggers T, Baas PC, van Dam GM. Surgeons lack predictive accuracy for anastomotic leakage in gastrointestinal surgery. *Int J Colorectal Dis.* 2009; 24(5):569–576. [PubMed: 19221768]
3. Hyman N, Manchester TL, Osler T, Burns B, Cataldo PA. Anastomotic leaks after intestinal anastomosis: it's later than you think. *Ann Surg.* 2007; 245(2):254–258. [PubMed: 17245179]
4. Van't Sant HP, Weidema WF, Hop WC, Oostvogel HJ, Contant CM. The influence of mechanical bowel preparation in elective lower colorectal surgery. *Ann Surg.* 2010; 251(1):59–63. [PubMed: 20009750]

5. Veyrie N, Ata T, Muscari F, Couchard AC, Msika S, Hay JM, Fingerhut A, Dziri C. Anastomotic leakage after elective right versus left colectomy for cancer: prevalence and independent risk factors. *J Am Coll Surg*. 2007; 205(6):785–793. [PubMed: 18035262]
6. Matsui A, Lee BT, Winer JH, Laurence RG, Frangioni JV. Predictive capability of near-infrared fluorescence angiography in submental perforator flap survival. *Plast Reconstr Surg*. 2010; 126(5): 1518–1527. [PubMed: 21042109]
7. Holm C, Tegeler J, Mayr M, Becker A, Pfeiffer UJ, Muhlbauer W. Monitoring free flaps using laser-induced fluorescence of indocyanine green: a preliminary experience. *Microsurgery*. 2002; 22(7):278–287. [PubMed: 12404345]
8. Pestana IA, Coan B, Erdmann D, Marcus J, Levin LS, Zenn MR. Early experience with fluorescent angiography in free-tissue transfer reconstruction. *Plast Reconstr Surg*. 2009; 123(4):1239–1244. [PubMed: 19337092]
9. Yamaguchi S, De Lorenzi F, Petit JY, Rietjens M, Garusi C, Giraldo A, Rey PC, Urban C, Martella S, Bosco R. The “perfusion map” of the unipedicled TRAM flap to reduce postoperative partial necrosis. *Ann Plast Surg*. 2004; 53(3):205–209. [PubMed: 15480004]
10. Rubben A, Eren S, Krein R, Younossi H, Bohler U, Wienert V. Infrared videoangiography of the skin with indocyanine green—rat random cutaneous flap model and results in man. *Microvasc Res*. 1994; 47(2):240–251. [PubMed: 8022322]
11. Lee BT, Matsui A, Hutteman M, Lin SJ, Winer JH, Laurence RG, Frangioni JV. Intraoperative near-infrared fluorescence imaging in perforator flap reconstruction: current research and early clinical experience. *J Reconstr Microsurg*. 2010; 26(1):59–65. [PubMed: 20027541]
12. Troyan SL, Kianzad V, Gibbs-Strauss SL, Gioux S, Matsui A, Oketokoun R, Ngo L, Khamene A, Azar F, Frangioni JV. The FLARE intraoperative near-infrared fluorescence imaging system: a first-in-human clinical trial in breast cancer sentinel lymph node mapping. *Ann Surg Oncol*. 2009; 16(10):2943–2952. [PubMed: 19582506]
13. Park PO, Haglund U, Bulkley GB, Falt K. The sequence of development of intestinal tissue injury after strangulation ischemia and reperfusion. *Surgery*. 1990; 107(5):574–580. [PubMed: 2159192]
14. Chiu CJ, McArdle AH, Brown R, Scott HJ, Gurd FN. Intestinal mucosal lesion in low-flow states. I. A morphological, hemodynamic, and metabolic reappraisal. *Arch Surg*. 1970; 101(4):478–483. [PubMed: 5457245]
15. Cooperman M, Martin EW Jr, Keith LM, Carey LC. Use of Doppler ultrasound in intestinal surgery. *Am J Surg*. 1979; 138(6):856–859. [PubMed: 159631]
16. Ando M, Ito M, Nihei Z, Sugihara K. Assessment of intestinal viability using a non-contact laser tissue blood flowmeter. *Am J Surg*. 2000; 180(3):176–180. [PubMed: 11084124]
17. Hirano Y, Omura K, Yoshida H, Ohta N, Hiranuma C, Nitta K, Nishida Y, Watanabe G. Near-infrared spectroscopy for assessment of tissue oxygen saturation of transplanted jejunal autografts in cervical esophageal reconstruction. *Surg Today*. 2005; 35(1):67–72. [PubMed: 15622467]
18. Yasumura M, Mori Y, Takagi H, Yamada T, Sakamoto K, Iwata H, Hirose H. Experimental model to estimate intestinal viability using charge-coupled device microscopy. *Br J Surg*. 2003; 90(4): 460–465. [PubMed: 12673749]
19. Tollefson DF, Wright DJ, Reddy DJ, Kintanar EB. Intraoperative determination of intestinal viability by pulse oximetry. *Ann Vasc Surg*. 1995; 9(4):357–360. [PubMed: 8527336]
20. Silverman DG, Hurford WE, Cooper HS, Robinson M, Brousseau DA. Quantification of fluorescein distribution to strangulated rat ileum. *J Surg Res*. 1983; 34(2):179–186. [PubMed: 6823110]
21. Freeman DE, Gentile DG, Richardson DW, Fetrow JP, Tulleners EP, Orsini JA, Cimprich R. Comparison of clinical judgment, Doppler ultrasound, and fluorescein fluorescence as methods for predicting intestinal viability in the pony. *Am J Vet Res*. 1988; 49(6):895–900. [PubMed: 2969692]
22. Gorey TF. The recovery of intestine after ischaemic injury. *Br J Surg*. 1980; 67(10):699–702. [PubMed: 7427023]
23. Gioux S, Choi HS, Frangioni JV. Image-guided surgery using invisible near-infrared light: fundamentals of clinical translation. *Mol Imaging*. 2010; 9(5):237–255. [PubMed: 20868625]



24. Kudsus S, Roesel C, Schachtrupp A, Hoer JJ. Intraoperative laser fluorescence angiography in colorectal surgery: a noninvasive analysis to reduce the rate of anastomotic leakage. *Langenbecks Arch Surg.* 2010; 395(8):1025–1030. [PubMed: 20700603]

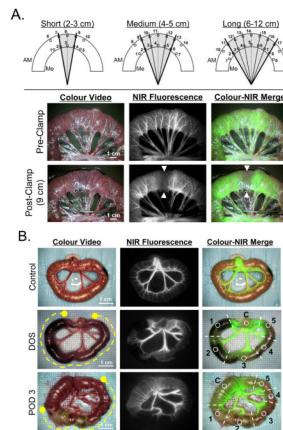


**Figure 1. Experimental preclinical models of bowel ischemia and NIR fluorescence angiography**

**A. Pig Model:** Various lengths of ischemic bowel sections (gray shading). ROIs of subsections on the mesenteric side (Me) and anti-mesenteric side (AM) were numbered as shown (see also Supplementary Tables S1 and S2). NIR fluorescence angiography before (pre-clamp) and after (post-clamp) induction of ischemia (arrowheads) via mesenteric vascular occlusion. The length of ischemia is 9 cm (long ischemic segment group). Shown are the colour video image (left), NIR fluorescence image (centre), and a pseudo-coloured (lime green) merged image of the two (right) at 1 min postinjection of 0.05-mg/kg ICG. Camera exposure time (60 ms) and normalizations are identical for NIR fluorescence images.

**B. Rat Model:** Typical NIR fluorescence angiography results seen under control conditions (Control; top) and intraoperatively after 2 h of strangulation on the day of surgery (DOS; middle row) and 3 days postoperatively (POD 3; bottom row). Shown are the colour video image (left), NIR fluorescence image (centre), and a pseudo-coloured (lime green) merged image of the two (right) at 40 s postinjection of 0.15-mg/kg ICG. The yellow dashed lines in the colour video mark the extent of strangulation. Camera exposure time (60 ms) and normalizations are identical for NIR fluorescence images. Each bowel was divided into 5 numbered sub-sections with a single ROI (circle) placed in each. An additional ROI was placed over normal bowel as a control (C).

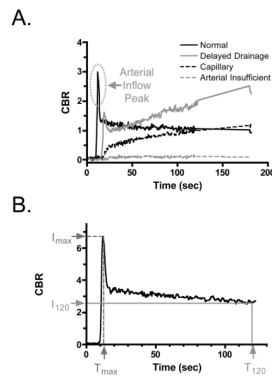


**Figure 2. Qualitative and quantitative metrics derived from NIR fluorescence angiography**  
 A. Qualitative patterns of vascular filling seen during the first 3 min after ICG injection. The arterial inflow peak seen under normal conditions is indicated.  
 B. Quantitative metrics were derived from the CBR at peak arterial inflow ( $I_{max}$ ) and its corresponding time ( $T_{max}$ ), and the plateau CBR seen at  $T = 120$  s ( $I_{120}$ ) after ICG injection. The drainage ratio (DR) is defined as  $I_{120}/I_{max} \times 100$ .

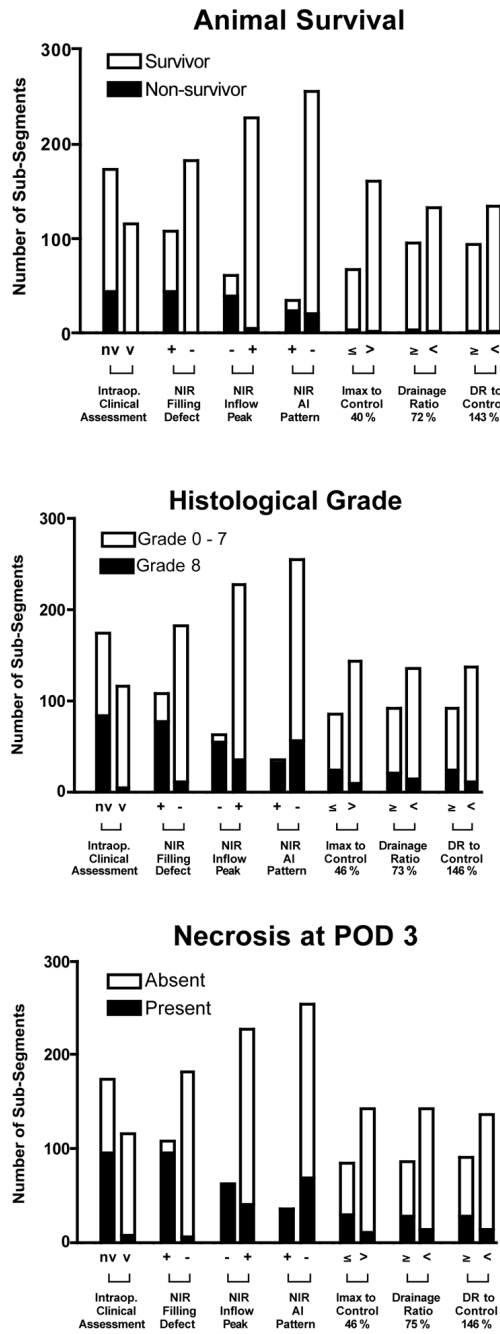


**Figure 3. Clinical outcomes as a function of clinical assessment, qualitative CBR-time curve metrics, and quantitative CBR-time curve metrics**  
 Shown are animal survival (top), histological grade (middle), and clinical necrosis on post-operative day 3 (bottom) as a function of the metrics shown and the number of bowel sub-segments involved. nv = nonviable, v = viable. + = feature present. - = feature absent.

**Table 1**

Predictive Capability of Clinical Assessment or Qualitative CBR-Time Curve Patterns for Survival, Histological Grade, and Tissue Necrosis on POD 3

	<b>Clinically Non-viable</b>	<b>NIR Filling Defect Present</b>	<b>NIR Inflow Peak Absent</b>	<b>AI Pattern Present</b>
<b>Animal Survival</b>				
Sensitivity	100%	97%	86%	53%
Specificity	47%	73%	90%	95%
Accuracy	55%	77%	90%	88%
<i>P</i> value *	< 0.0001	< 0.0001	< 0.0001	< 0.0001
Odds Ratio (CI 95%)	81.86 (4.984–1345)	124.4 (16.79–922.2)	62.74 (24.00–164.0)	24.31 (10.47–56.43)
<b>Histological Grade</b>				
Sensitivity	94%	87%	60%	35%
Specificity	55%	85%	96%	98%
Accuracy	67%	85%	85%	79%
<i>P</i> value *	< 0.0001	< 0.0001	< 0.0001	< 0.0001
Odds Ratio (CI 95%)	20.72 (8.059–53.27)	40.42 (19.26–84.81)	37.22 (16.30–84.97)	37.05 (10.94–125.5)
<b>Clinical Necrosis</b>				
Sensitivity	93%	92%	60%	33%
Specificity	58%	93%	100%	100%
Accuracy	70%	92%	85%	76%
<i>P</i> value *	< 0.0001	< 0.0001	< 0.0001	< 0.0001
Odds Ratio (CI 95%)	19.16 (8.435–43.55)	156.6 (89.50–747.7)	564.8 (34.21–9323)	194.3 (11.75–3214)

\* Fisher exact test. AI Pattern = arterial insufficiency pattern; CI 95% = confidence interval of 95%.



**Table 2**

Predictive Capability of Quantitative CBR-Time Parameters for Survival, Histological Grade, and Tissue Necrosis on POD 3

	<b>I<sub>max</sub> to Control (%)</b>	<b>Drainage Ratio (DR) (%)</b>	<b>DR to Control (%)</b>
<b>Animal Survival</b>			
Cutoff Value	40%	72%	143%
Area Under ROC Curve	0.7463	0.6788	0.6067
Sensitivity	67%	67%	50%
Specificity	72%	59%	59%
Accuracy	71%	59%	59%
<i>P</i> value*	0.0631	0.2376	0.6926
Odds Ratio ( <i>CI</i> 95%)	5.048 (0.9014–28.26)	2.879 (0.5162–16.06)	1.44 (0.2841–7.295)
<b>Histological Grade</b>			
Cutoff Value	46%	73%	146%
Area Under ROC Curve	0.7823	0.6631	0.8409
Sensitivity	72%	60%	69%
Specificity	69%	63%	65%
Accuracy	69%	62%	66%
<i>P</i> value*	< 0.0001	0.0145	0.0003
Odds Ratio ( <i>CI</i> 95%)	5.858 (2.570–13.35)	2.556 (1.223–5.343)	4.103 (1.894–8.888)
<b>Clinical Necrosis</b>			
Cutoff Value	46%	75%	146%
Area Under ROC Curve	0.7956	0.7547	0.7450
Sensitivity	73%	68%	66%
Specificity	71%	69%	66%
Accuracy	71%	69%	66%
<i>P</i> value*	< 0.0001	< 0.0001	0.0003
Odds Ratio ( <i>CI</i> 95%)	6.545 (3.063–13.99)	4.79 (2.315–9.914)	3.706 (1.817–7.561)

\* Fisher exact test. ROC curve = receiver operating characteristic curve; *CI* 95% = confidence interval of 95%.